



## Computational study on the inhibition mechanism of cruzain by nitrile-containing molecules

Oscar Méndez-Lucio<sup>a</sup>, Antonio Romo-Mancillas<sup>a</sup>, José L. Medina-Franco<sup>b</sup>, Rafael Castillo<sup>a,\*</sup>

<sup>a</sup> Facultad de Química, Departamento de Farmacia, Universidad Nacional Autónoma de México, México 04510, D.F., Mexico

<sup>b</sup> Torrey Pines Institute of Molecular Studies, 11350 SW Village Parkway, Port St. Lucie, FL 34987, USA

### ARTICLE INFO

#### Article history:

Received 25 October 2011

Received in revised form 6 January 2012

Accepted 10 January 2012

Available online 20 January 2012

#### Keywords:

Cruzain

Cysteine proteases

Density functional theory

Semi-empirical quantum mechanics

*Trypanosoma cruzi*

### ABSTRACT

Cysteine proteases from parasites as well as from mammals are promising drug targets for parasitic infections and systemic human diseases, respectively. Many reversible and irreversible inhibitors of this very large class of proteins have been designed. Among others, molecules with a nitrile moiety, which is a group that is susceptible to a nucleophilic attack by the enzyme, have been identified as good inhibitors. Although it is known that the nitrile group binds covalently to Cys25, there are no reports about the energetics involved in the mechanism of this process. Herein, density functional theory and quantum semi-empirical calculations were conducted in order to study the molecular recognition of cysteine proteases by nitrile-containing molecules. Results reported in this paper suggest an interaction that starts with a nucleophilic attack from the Cys25 to the inhibitor followed by a proton transfer from His162. Only one transition state was detected; however, we found the existence of an energy plateau in the potential energy surface. Based on the proposed mechanism, some structural features that could improve the biological activity of nitrile-containing molecules toward cysteine proteases are discussed.

© 2012 Elsevier Inc. All rights reserved.

### 1. Introduction

Cysteine proteases are involved in many biological processes. The misregulation of these enzymes conduces to a variety of diseases; therefore, they represent promising drug targets [1,2]. The huge class of cysteine proteases are divided into 20 families and grouped into three clans. Clan A comprises the C1, C2 and C10 families, which can be described as “papain-like proteases” [3]. Cysteine proteases from parasites as well as from mammals that belong to this clan are promising drug targets for parasitic infections and systemic human diseases [2]. For example, cathepsins B, F, K and L are involved in rheumatoid arthritis, cancer, osteoporosis and atherosclerosis, while falcipain, cruzain, and rhodesain are drug targets against malaria (*Plasmodium falciparum*), Chagas’ disease (*Trypanosoma cruzi*) and sleeping sickness (*Trypanosoma brucei*), respectively [1,2].

The active site of the cysteine proteases is composed of the catalytic triad Cys25, His162, and Asn182 (cruzain numbering) [4]. The proposed mechanism for this triad operates as follows: Asn182 acts as a hydrogen bond acceptor toward the His162, enabling the formation of a permanent imidazolium–thiolate ion pair between Cys25 and His162 [5]. It has been proposed that another

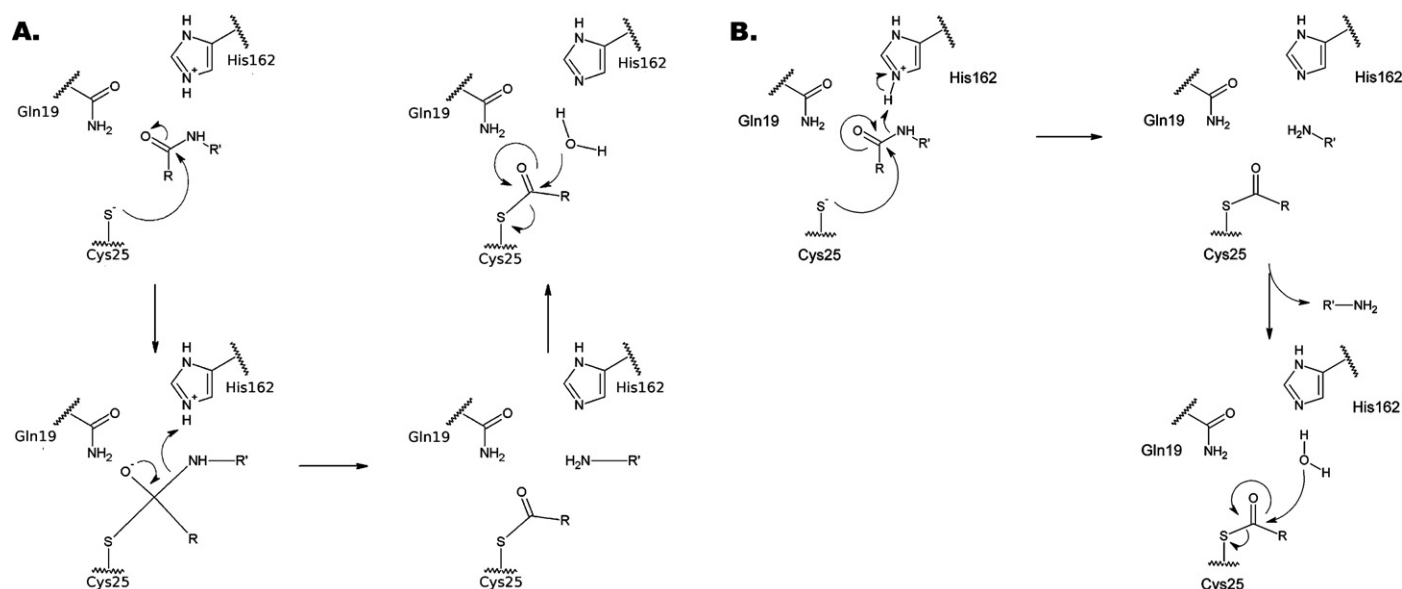
important amino acid in the catalytic site is Gln19, which acts as part of an oxyanion hole that stabilizes an acyl-enzyme intermediate by forming a hydrogen bond between the amino group in the Gln19 and the substrate [6].

Two main catalytic mechanisms of enzymatic activity of cysteine proteases have been proposed. The former consists of a serine protease-like mechanism proposed by Drenth et al. [7] that takes place in three steps (Scheme 1A). The first step is the nucleophilic attack on the substrate by the thiolate. A stabilization of the transition state in this reaction occurs by the hydrogen bond between the substrate and the backbone NH of Cys25. The resulting tetrahedral intermediate is stabilized by a hydrogen bond formed between Gln19 in the oxyanion hole and the ligand. The latter is a proton transfer from the imidazolium ion to the nitrogen of the amide in the substrate to form an acyl-enzyme complex. Finally, the deacylation occurs via a water molecule which attacks the acyl-enzyme complex at the carbonyl carbon to produce the final products [7]. An alternative mechanism has been proposed in which the protonation of the oxygen or nitrogen in the substrate caused by a proton transfer from His162 must occur prior, or in a concerted manner, to the nucleophilic attack [8–10].

A wide range of peptidic or non-peptidic molecules with a group susceptible to a nucleophilic attack can inhibit cysteine proteases. For example, vinyl sulfones, fluoro methyl ketones, aziridines or nitriles have shown good inhibition activity [1,2]. Nevertheless, the inhibition mechanism of only a few of them has been studied, both

\* Corresponding author. Tel.: +52 5 56 22 52 87; fax: +52 5 56 22 53 29.

E-mail addresses: [rafaelc@unam.mx](mailto:rafaelc@unam.mx), [rafaelc@servidor.unam.mx](mailto:rafaelc@servidor.unam.mx) (R. Castillo).



**Scheme 1.** (A) Serine protease-like catalytic mechanism proposed for cysteine proteases. (B) Alternative catalytic mechanism in which the proton transfer occurs prior, or in a concerted manner, to the nucleophilic attack.

experimentally and theoretically [11–15]. Further advances in theoretical methods should facilitate mechanistic studies that could result in new inhibitor classes [16].

Cruzain is the major cysteine protease of *T. cruzi*, the causal agent of Chagas' disease, and has been identified as an important enzyme for the parasite survival on the host [17,18]. Because of the biological importance of cruzain, many attempts to inhibit this enzyme have been undertaken. Recently, the inhibitor 6-[(3,5-difluorophenyl)amino]-9-ethyl-9H-purine-2-carbonitrile (Table 1) was identified as an inhibitor of cruzain with an  $IC_{50}$  of 0.01  $\mu$ M [19]. As stated above, molecules with a nitrile moiety have been used as a reversible covalent inhibitor of cysteine proteases [1,2], although their inhibition mechanism has not yet been studied from a computational perspective. For this reason, the principal aim of this paper is to gain insights into the mechanism whereby the nitrile inhibitors bind to cysteine proteases, especially to cruzain. Density functional theory and quantum semi-empirical calculations were employed to analyze the energy profile of the putative mechanism of inhibition of cruzain. This paper is part of our on going efforts to rationalize, at the molecular level, the structure–activity relationships and mechanism of inhibition of purine-carbonitriles that serve as guide to design new inhibitors of cruzain [20].

## 2. Computational methods

### 2.1. Density functional theory calculations

For these calculations an isolated model including the side chains of two residues (Cys25 and His162) and a purine-carbonitrile as a model of the inhibitors were used (shown in Table 1). The methyl groups corresponding to the protein backbone were the only atoms fixed in these calculations. A three-dimensional representation of the protein model used for these calculations is depicted in Fig. 1.

A search along the potential energy surface of the binding recognition of cruzain by a purine-carbonitrile was performed using the B3LYP hybrid functional [21,22] with the 6-31+G(d) basis set. The stationary point corresponding to a transition state was characterized by an imaginary frequency resulting from the

harmonic vibrational frequency calculations. On the other hand, reactants and products were confirmed by the absence of imaginary frequencies. Intrinsic reaction coordinate calculations (using a step size of 0.13 Bohr) were performed to confirm the connectivity between the transition state and the desired reactants and products. Single-point calculations were computed at M05-2X/6-31+G(d)//B3LYP/6-31+G(d) level of theory for all the IRC and stationary points, as proposed by Goodman and co-worker after a benchmark study [23]. Since the catalytic site of the cruzain is located in an external region of the protein, which is exposed to solvent, a polarizable continuum model (PCM) was used applying the integral equation formalism variant (IEFPCM) with water as solvent during all the calculations. All calculations were carried out using Gaussian09 software [24].

Fukui indices [25], which were computed in order to assess reactive sites within a molecule, can be defined as:

$$f^-(r) = \left( \frac{\partial \rho(r)}{\partial N} \right)_v^- = \rho_{N_0}(r) - \rho_{N_0-1}(r)$$

$$f^+(r) = \left( \frac{\partial \rho(r)}{\partial N} \right)_v^+ = \rho_{N_0+1}(r) - \rho_{N_0}(r)$$

and

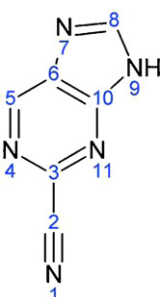
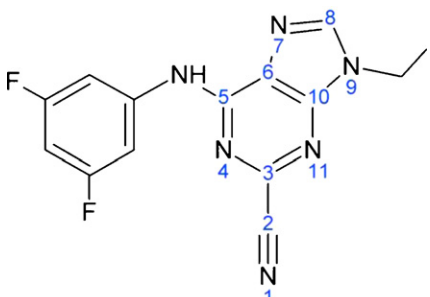
$$f^0(r) = \left( \frac{\partial \rho(r)}{\partial N} \right)_v^0 = \frac{1}{2}(f^-(r) + f^+(r)) = \frac{1}{2}(\rho_{N_0+1}(r) - \rho_{N_0-1}(r))$$

where  $\rho_{N_0-1}$ ,  $\rho_{N_0}$ , and  $\rho_{N_0+1}$  are the electron densities of the  $N_0 - 1$ ,  $N_0$ , and  $N_0 + 1$  electron systems. The function  $f^-(r)$  defines the place where the removal of a fraction of electron is more energetically favorable, while  $f^+(r)$  defines the place where it is more favorable to add it. In terms of reactivity, large values of  $f^-(r)$  would indicate a good nucleophile; on the other hand, large values of  $f^+(r)$  highlight susceptible areas for a nucleophilic attack [26].

### 2.2. Quantum semi-empirical calculations

In order to investigate possible interactions between inhibitors with a nitrile group and the active site of cruzain, the crystallographic structure of cruzain co-crystallized with the

**Table 1**  
Calculated Fukui function values computed at B3LYP/6-31+G(d).

Atom	NBO			Mulliken			NBO			Mulliken		
	$f_A^+$	$f_A^-$	$f_A^0$	$f_A^+$	$f_A^-$	$f_A^0$	$f_A^+$	$f_A^-$	$f_A^0$	$f_A^+$	$f_A^-$	$f_A^0$
N1	-0.18	-0.203	-0.191	-0.174	-0.181	-0.177	-0.154	-0.089	-0.121	-0.149	-0.085	-0.117
C2	0.018	0.01	0.014	-0.007	-0.015	-0.011	0.008	0.032	0.020	0.007	0.001	0.004
C3	-0.127	-0.113	-0.120	-0.072	-0.05	-0.061	-0.118	-0.031	-0.074	-0.055	0.029	-0.013
N4	-0.018	-0.042	-0.030	-0.068	-0.096	-0.082	0.000	-0.034	-0.017	-0.049	-0.04	-0.044
C5	-0.144	-0.079	-0.111	-0.146	-0.033	-0.089	-0.094	0.029	-0.032	-0.025	0.041	0.008
C6	-0.056	-0.09	-0.073	-0.078	-0.087	-0.082	-0.046	-0.062	-0.054	-0.039	-0.036	-0.037
N7	-0.05	-0.095	-0.072	-0.064	-0.125	-0.094	-0.031	-0.016	-0.023	-0.055	-0.042	-0.048
C8	-0.143	-0.136	-0.139	-0.106	-0.066	-0.086	-0.118	-0.069	-0.093	-0.129	-0.038	-0.083
N9	-0.024	-0.013	-0.018	-0.011	-0.041	-0.026	-0.029	-0.015	-0.022	0.027	-0.004	0.011
C10	-0.003	-0.063	-0.033	0.053	-0.009	0.022	-0.003	-0.03	-0.016	0.001	-0.031	-0.015
N11	-0.155	-0.056	-0.105	-0.157	-0.11	-0.133	-0.114	-0.081	-0.097	-0.116	-0.092	-0.104

inhibitor 6-[(3,5-difluorophenyl)amino]-9-ethyl-9H-purine-2-carbonitrile (Table 1) was obtained from the Protein Data Bank (PDB ID: 3I06) [19].

The potential energy surface for this reaction was mapped by scanning two different reaction coordinates at the same time: the distances C2–S and N1–H. These atoms were approached and geometry optimizations were carried out every 0.05 Å using the PM6 quantum semi-empirical method. A similar methodology has been used before studying different enzyme reaction mechanisms [27–30].

Since the aim of this paper is to study a reaction that takes place in the catalytic site of the enzyme, 275 atoms in the active site and 32 atoms in the ligand were explicitly treated by the PM6 quantum semi-empirical method. The calculations were prepared using TRITON, a free access software that acts as a graphic user interface for MOPAC and other programs [31]. The calculations were carried out using only a cavity formed by 20 amino acids in the active site (Gln19, Cys22, Gly23, Ser24, Cys25, Trp26, Cys63, Ser64, Gly65, Gly66, Leu67, Met68, Val137, Ala138, Val139, Leu160, Asp161, His162, Gly163, Glu208), as shown in Fig. 1. For these amino acids, the backbone atoms were fixed through all the calculations and all the side chains and ligand atoms were optimized using the BFGS method [32–35].

All the calculations were conducted with MOPAC2009 software for semi-empirical calculations employing the PM6 Hamiltonian for all atoms and the localized molecular orbital method MOZYME [36–40]. A continuum COSMO model with the water dielectric constant of 78.4 was used in all the semi-empirical calculations [41].

### 3. Results and discussion

#### 3.1. Potential energy surface

The potential energy surface (PES) of the binding recognition of cruzain by a purine-carbonitrile was studied using DFT calculations. A low-energy reaction pathway was found when the inhibitor approaches the thiolate of Cys25 starting a nucleophilic attack. This result is not surprising since the carbon of the nitrile has a charge deficit that enhances the nucleophilic attack from the thiolate. The

PES of this inhibition is shown in Fig. 2, and it can be seen that the reactants must surpass an energetic barrier no higher than 1.39 kcal/mol. The transition state is reached at a C2–S distance of 2.39 Å. In this structure the thiolate interacts with the carbon of the nitrile; this interaction produces an electron migration from the carbon to the *p* orbital of the thiolate making the N1–C2 bond of the nitrile weaker. This fact is reflected in the elongation of the N1–C2 distance up to 1.19 Å at the same time as the triple bond of the nitrile breaks to form a double bond. Interestingly, the interaction between the N1 and H atoms seem to be relatively weak since they are separated by 1.78 Å.

After the transition state, an unusual energy plateau related to the hydrogen transfer from the His162 to the nitrile moiety can be observed. The calculated Fukui function value  $f_A^+ = 0.180$  (Table 1) indicates that a negative charge added to the purine-carbonitrile will be located on the nitrogen of the nitrile. An increased charge in the nitrile makes the nitrogen a good nucleophile ( $f_A^-$  value of 0.203) thus facilitating the proton transfer from the histidine to the inhibitor. Moreover, in the energy plateau the dihedral angle S–C2–C3–N11 starts to change in order to conjugate the  $\pi$  electrons of the N1–C2 double bond with those of the purine ring. This kind of PES that presents an energy plateau near the transition state has been observed before and it may be consequence of the vibronic interactions that prevail in this region [42]. Vibronic interactions are favored by low-lying excited states that become very important near transition states, where different electronic states may cross. Although the crossing of the two surfaces is prevented by the vibronic interactions which tend to maximize the gap between them, they frequently cause the flattening of the lower one [42]. It is important to mention that the C2–S distance does not change significantly at the plateau and is not short enough to complete the formation of a covalent bond. The structures of the stationary points are depicted in Fig. 3. Some geometrical parameters and the energetics of the reaction are listed in Table 2.

As the reaction coordinate increases, the PES reaches the edge of the energy plateau and from this point on, the PES follows a downhill path up to the final product, a thioimide, which lies 22.07 kcal/mol below the energy of the reactants. The difference in energy between the reactants and the product is due to two

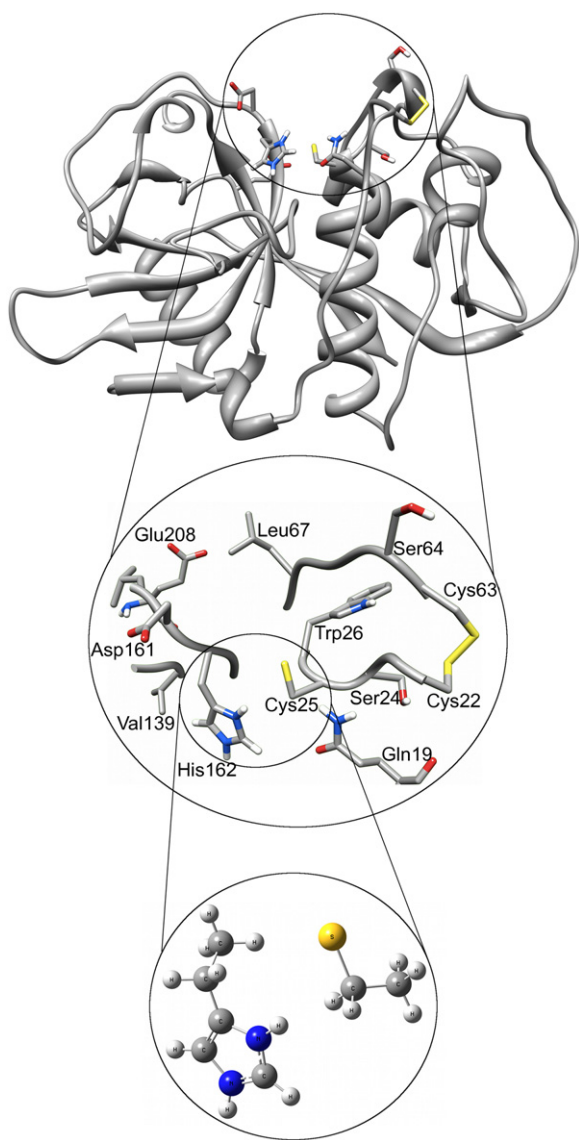


**Fig. 1.** Crystallographic structure of cruzain (PDB ID: 3I06) used in this study (top). The model used during the semi-empirical calculations is shown in the middle and the one used in DFT calculations is shown at the bottom.

factors: the formation of a chemical bond between the sulfur atom of Cys25 and the carbon on the nitrile, and the stabilization of the bond between the proton and the nitrogen of the ligand. In the resulting thioimide, the bond lengths of C2–S, N1–C2 and N1–H are 1.81, 1.27, 1.02 Å, respectively; it has a N1–C2–C3 angle of 119.82° and a dihedral S–C2–C3–N11 angle of 153.34°.

It is known that the nitrile-containing molecules form a reversible thioimide ester adduct between the inhibitor and the active site of the enzyme, in this case, the Cys25 [43]. Based on the PES, we can say that this interaction is reversible at the energy plateau and before the edge is reached; in other words, before the proton transfer from His162 is completed. This is an important observation as it would be interesting to modulate the reversibility of this interaction.

In order to analyze how the substituents on the purine scaffold could affect the reactivity toward the cysteine protease, we computed the stationary points of the co-crystal inhibitor 6-[(3,5-difluorophenyl)amino]-9-ethyl-9H-purine-2-carbonitrile which has an  $IC_{50}$  of 0.01  $\mu$ M against cruzain [19]. Interestingly, neither the relative energy nor the structural parameter differs from those

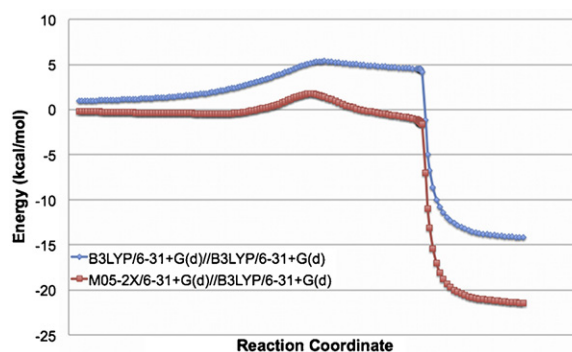


**Fig. 2.** Potential energy surfaces obtained for the inhibition of cruzain by a purine-carbonitrile.

of the purine-carbonitrile (Table 2). This result suggests that at least these substituents do not have an important effect on the reactivity of the nitrile group; nonetheless, it would be interesting to study inhibitors with electron withdrawing and electron donor groups directly bound to the purine ring and their influence on the reactivity and biological activity.

Using these results as a guideline for drug design, it can be suggested that the reversibility of carbonitrile inhibitors could be regulated by reducing or increasing the negative charge in the nitrile nitrogen. A reduced negative charge on this nitrogen would delay the proton transfer causing a more reversible interaction. On the other hand, an increased negative charge on the nitrogen would facilitate the formation of the thioimide. Besides, the energetic barrier could be reduced by increasing the electrophilicity of the carbon on the nitrile in order to facilitate the nucleophilic attack from the Cys25 thiolate.

### 3.2. Molecular orbitals analysis

A useful model to assess and analyze reactivity is the molecular orbital model, especially the frontier orbital approach. This approach is based on the assumption that a bond formation is caused by the flow of electrons from the highest occupied molecular orbital (HOMO) to the lowest unoccupied molecular orbital (LUMO).

HOMO and LUMO of the stationary points are depicted in Fig. 4. The HOMO–LUMO energy gap of the reactants is 50.88 kcal/mol, indicating that the reaction may take place with a low energetic barrier. The HOMO of the reactants is localized on a cysteine, mainly at the  $p$  orbital of the thiolate, which acts as an electron donor. On the other hand, the LUMO is formed by the  $p$  orbital system in the purine. Since these two  $p$  orbitals must interact, it is necessary that the nucleophilic attack from the thiolate proceed perpendicularly to the plane that contains the purine ring. It is important to highlight that a stereochemical feature arises because the nucleophile is free to attack from either side of the plane. Nevertheless, the more favorable interaction is at the moment the attack proceeds when the C5 in the purine is pointing to the His162, since this interaction is allowed by orbital symmetry.

Analyzing the HOMO of the next step of the reaction, the transition state, it can be noticed that the  $p$  orbitals localized on the purine and the cysteine overlap because of the electron transfer from the S to the C2, and they start the formation of a chemical bond. A detail that stands out is the  $p$  orbital of the nitrile nitrogen, which points to the histidine hydrogen but is overlapped with the  $s$  orbital of the cysteine side chain hydrogen. An issue that must be addressed is that the nitrile is bonded to the purine ring by the interaction of an  $s$  orbital.



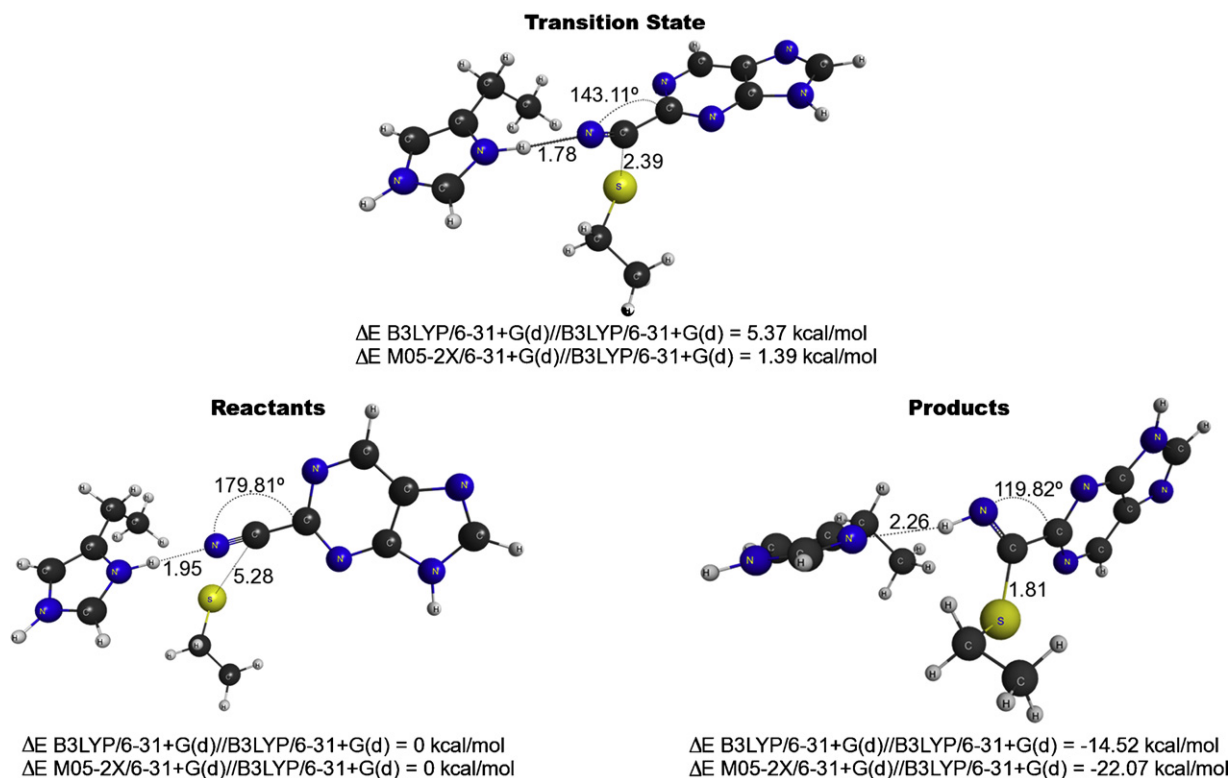


Fig. 3. Optimized structures of the stationary points at B3LYP/6-31+G(d) level of theory. The distances and bond lengths are indicated in Å.

Finally, the products of the reaction are characterized by a large HOMO–LUMO energy gap of 97.72 kcal/mol, which is related to the high stability of the products. Although the frontier orbitals of the products are not as interesting as those of the reactants or transition state, it can be seen in Fig. 4 that these HOMO and LUMO cannot react with each other, favoring the stability of the products. The HOMO of the products is located mainly in the *p* orbital system of the imidazole in the histidine, while the LUMO is composed by antibonding *p* orbitals in the purine.

### 3.3. Reaction inside the active site

Since it is possible that other amino acids, different from the catalytic ones, could take part in the inhibition reaction by stabilizing the transition state or products, in this section the role of other amino acids in the catalytic site during the molecular interaction was studied. For this purpose, quantum

semi-empirical calculations were carried out in order to analyze possible interactions between the inhibitor and the active site of the enzyme during the reaction; specifically, the PES of the cruzain inhibition by 6-[(3,5-difluorophenyl)amino]-9-ethyl-9H-purine-2-carbonitrile was mapped. Two reaction coordinates were followed inside a cavity of 20 amino acids of the cruzain catalytic active site: the C2–S distance between thiolate and the nitrile; and the N1–H distance between the nitrile and histidine. The 2D PES obtained from these calculations is depicted in Fig. 5. It can be seen that the lowest energy pathway is the one in which the S and the C2 approach in such a way that seems to be a nucleophilic attack. Once the S and the C2 are close enough, a proton migration from the histidine to the nitrogen nitrile occurs so that the final products may be reached. On the other hand, no energetically favored pathway was found for the process in which the protonation of the nitrile takes place before the nucleophilic attack from the thiolate; in fact, this is a very disfavored process, as shown in Fig. 5.

Table 2  
Selected geometrical parameters and energetics for the stationary points in the inhibition of cruzain.

Parameters	Purine-carbonitrile			6-[(3,5-Difluorophenyl)amino]-9-ethyl-9H-purine-2-carbonitrile		
	Reactants	Transition state	Products	Reactants	Transition state	Products
<i>r</i> (N1–C2)	1.1601	1.1920	1.2723	1.1602	1.1926	1.2727
<i>r</i> (N1–H)	1.9514	1.7763	1.0279	1.9441	1.7552	1.0266
<i>r</i> (N1–N <sub>HIS</sub> )	2.9749	2.8221	3.1898	2.9705	2.8063	3.2256
<i>r</i> (C2–C3)	1.4492	1.4742	1.5048	1.4509	1.4774	1.5075
<i>r</i> (C2–S)	5.2787	2.3900	1.8143	5.1646	2.3829	1.8128
<i>r</i> (N <sub>HIS</sub> –H)	1.0276	1.0488	2.2601	1.0284	1.0531	2.3212
$\theta$ (N1–C2–C3)	179.811	143.108	119.817	179.624	142.394	119.885
$\theta$ (N1–C2–S)	52.949	118.651	127.363	56.049	118.496	127.361
$\theta$ (H–N1–C2)	178.611	127.319	113.715	178.490	130.261	113.607
<i>D</i> (S–C2–C3–N11)	–62.592	–108.634	–153.342	–73.239	–109.024	–154.944
<i>D</i> (S–C2–N1–H)	162.889	–36.166	–5.877	–13.455	–25.275	–5.609
<i>E</i> (B3LYP/6-31+G(d)//B3LYP/6-31+G(d))	0.00	5.37	–14.52	0.00	6.27	–13.94
<i>E</i> (M05-2X/6-31+G(d)//B3LYP/6-31+G(d))	0.00	1.39	–22.07	0.00	1.50	–22.42

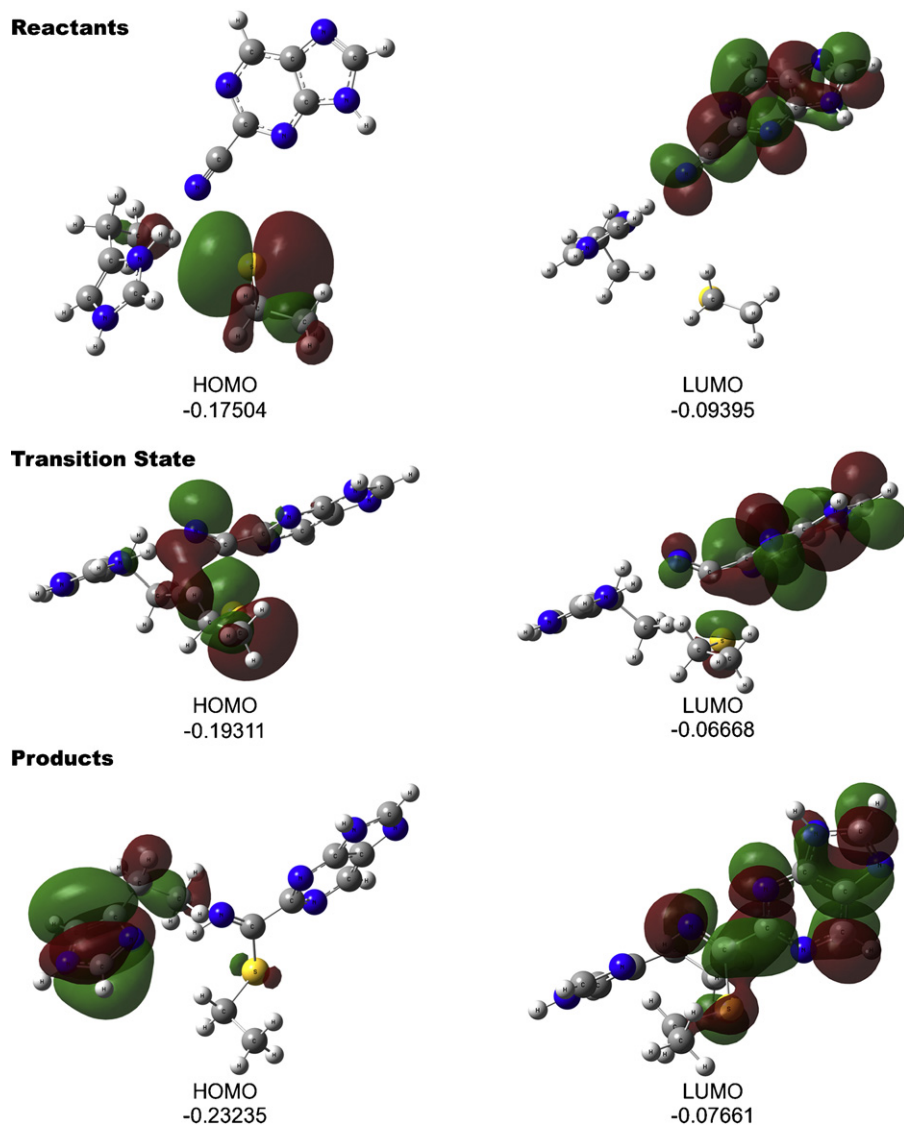


Fig. 4. B3LYP frontier molecular orbitals and orbital energies (in atomic units) of the stationary points.

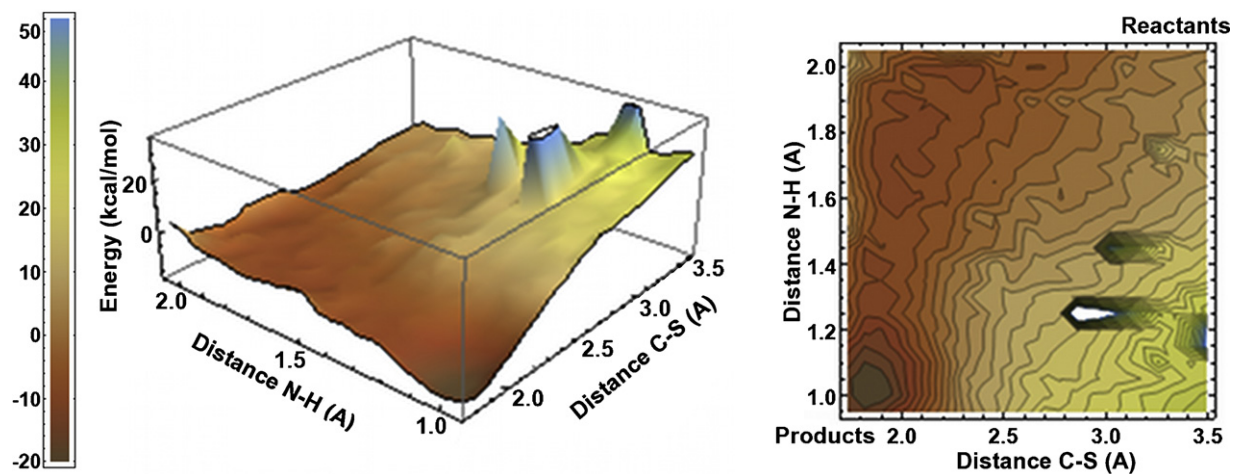


Fig. 5. 2D potential energy surface for the inhibition of cruzain computed with the PM6 Hamiltonian.

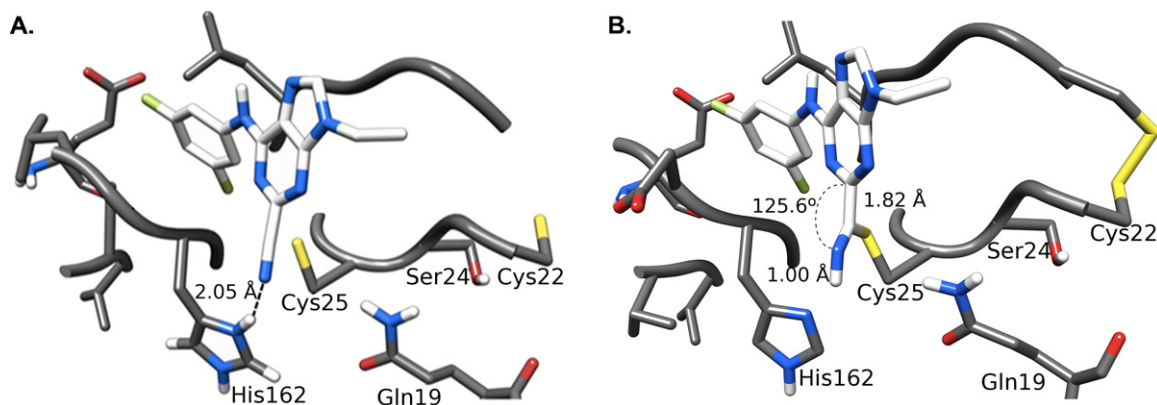


Fig. 6. Optimized structures of reactants (A) and products (B) employing the PM6 Hamiltonian.

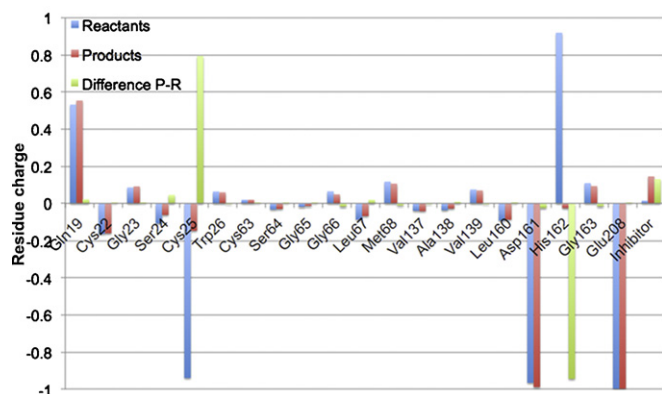


Fig. 7. Histogram showing the charge variation of 20 amino acids in the active site during the reaction.

The results obtained using quantum semi-empirical methods are in good agreement with the DFT calculations. This fact is reflected by the resulting reaction pathway for this process and by the relative energy of the products, which is 17.07 kcal/mol below the reactants. Also, the geometrical parameters are very similar to those of the structures optimized using DFT; for example, the C2–S, N1–C2 and N1–H bond lengths are 1.82, 1.26, 1.00 Å, respectively; the N1–C2–C3 angle is 125.60° and the dihedral S–C2–C3–N11 angle is 134.50° (Fig. 6).

The variation of the total Mulliken charge on the amino acid residue was used to assess possible interactions during the reaction. The residue charge was calculated as the sum of partial charges from all its atoms. The charge variation between reactants and products is shown in Fig. 7. It can be seen that most of the residues do not present any significant charge variation. Nonetheless, as was expected, the two amino acids that take part in the reaction (Cys25 and His162) presented a charge variation due to the proton transfer. A fact that must be highlighted is that Gln19, which acts as part of an oxyanion hole, has a low variation of the positive charge during the reaction. This could be indicative of the fact that the Gln19 does not play a major role in the stabilization of the inhibitor.

#### 4. Conclusions and perspectives

A theoretical study, using DFT and quantum semi-empirical calculations, was carried out to reveal the mechanism of the inhibition of cysteine proteases by nitriles. This paper shows evidence suggesting that the inhibition occurs via a mechanism which starts with a nucleophilic attack from the Cys25 to the inhibitor followed by a proton transfer from the His162. The reaction presents a very

particular PES that consists of one transition state and an energy plateau. These results are in good agreement with the proposed peptide hydrolysis mechanism of papain, another cysteine protease, in which the peptide hydrolysis occurs in a concerted manner [8–10]. On the other hand, no intermediates were found as had been in the models for the inhibition of cysteine proteases by diketones, halomethyl ketones, diazomethyl ketones and aziridines [11–15].

Results presented in this paper suggest that the reversibility of this interaction could be managed by modulating the proton transfer from the His162 to the inhibitor. Additionally, an increased electrophilicity in the carbon on the nitrile might facilitate the nucleophilic attack from Cys25; in this way, the activation energy would be reduced at the same time as the inhibition activity would increase. This study presents information that is helpful for a better understanding of the mechanism of inhibition of cruzain by nitriles. The data obtained is useful for the design of better cysteine protease inhibitors that could lead to new trypanocidal agents. Future work is focused on studying the effect of different substituents in the purine scaffold on the energy profile of the reaction. A second perspective is to investigate how the reactivity and reversibility of the inhibitors could be modulated in order to design safe and effective drugs against Chagas' disease.

#### Acknowledgments

Authors are grateful to Karina Martinez-Mayorga for helpful discussions. This research was supported by CONACyT project No. 80093. O. M-L and A. R-M are very grateful to CONACyT for the fellowships granted (Nos. 245408 and 173861, respectively). J. L. M-F thanks the State of Florida for funding.

#### References

- [1] H.H. Otto, T. Schirmeister, Cysteine proteases and their inhibitors, *Chem. Rev.* 97 (1997) 133–172.
- [2] F. Lecaille, J. Kaleta, D. Brömme, Human and parasitic papain-like cysteine proteases: their role in physiology and pathology and recent developments in inhibitor design, *Chem. Rev.* 102 (2002) 4459–4488.
- [3] N.D. Rawlings, A.J. Barrett, Families of cysteine peptidases, *Methods Enzymol.* 244 (1994) 461–486.
- [4] M. McGrath, A. Eakin, J. Engel, J. McKerrow, C. Craik, R. Fletterick, The crystal structure of cruzain: a therapeutic target for Chagas' disease, *J. Mol. Biol.* 247 (1995) 251–259.
- [5] J. Nishihira, H. Tachikawa, Theoretical evaluation of a model of the catalytic triads of serine and cysteine proteases by ab initio molecular orbital calculation, *J. Theor. Biol.* 196 (1999) 513–519.
- [6] E. Dufour, A. Storer, R. Menard, Peptide aldehydes and nitriles as transition state analog inhibitors of cysteine proteases, *Biochemistry* 34 (1995) 9136–9143.
- [7] J. Drenth, K.H. Kalk, H.M. Swen, Binding of chloromethyl ketone substrate analogues to crystalline papain, *Biochemistry* (1976) 1–8.
- [8] D. Arad, R. Langridge, P. Kollman, A simulation of the sulfur attack in catalytic pathway of papain using molecular mechanics and semiempirical quantum mechanics, *J. Am. Chem. Soc.* 112 (1990) 491–502.

- [9] W. Welsh, Y. Lin, Discussion of the catalytic pathway of cysteine proteases based on AM1 calculations, *J. Mol. Struct.: Theochem.* 401 (1997) 315–326.
- [10] M. Harrison, N. Burton, I. Hillier, Catalytic mechanism of the enzyme papain: predictions with a hybrid quantum mechanical/molecular mechanical potential, *J. Am. Chem. Soc.* 119 (1997) 12285–12291.
- [11] M. Tarnowska, S. Oldziej, A. Liwo, P. Kania, F. Kasprzykowski, Z. Grzonka, MNDO study of the mechanism of the inhibition of cysteine proteinases by diazomethyl ketones, *Eur. Biophys. J.* 21 (1992) 217–222.
- [12] R. Shankar, P. Kolandaivel, K. Senthilkumar, Reaction mechanism of cysteine proteases model compound HSH with diketone inhibitor  $\text{PhCOCOCH}_3\text{-nXn}$  ( $\text{X}=\text{F}, \text{Cl}, n=0, 1, 2$ ), *Int. J. Quantum Chem.* 110 (2010) 1660–1674.
- [13] S. Vijayakumar, P. Kolandaivel, Reaction mechanism of HSH and  $\text{CH}_3\text{SH}$  with  $\text{NH}_2\text{CH}_2\text{COCH}_2\text{X}$  ( $\text{X}=\text{F}$  and  $\text{Cl}$ ) molecules, *Int. J. Quantum Chem.* 108 (2008) 927–936.
- [14] G. Barreiro, R. De Alencastro, J. Neto, A semiempirical study on leupeptin: an inhibitor of cysteine proteases, *Int. J. Quantum Chem.* 65 (1997) 1125–1134.
- [15] R. Vicik, H. Helten, T. Schirmeister, B. Engels, Rational design of aziridine-containing cysteine protease inhibitors with improved potency: studies on inhibition mechanism, *ChemMedChem* 1 (2006) 1021–1028.
- [16] M.K. Lindvall, Molecular modeling in cysteine protease inhibitor design, *Curr. Pharm. Des.* 8 (2002) 1673–1681.
- [17] J. Cazzulo, V. Stoka, V. Turk, The major cysteine proteinase of *Trypanosoma cruzi*: a valid target for chemotherapy of Chagas disease, *Curr. Pharm. Des.* 7 (2001) 1143–1156.
- [18] J.C. Engel, P.S. Doyle, I. Hsieh, J.H. McKerrow, Cysteine protease inhibitors cure an experimental *Trypanosoma cruzi* infection, *J. Exp. Med.* 188 (1998) 725–734.
- [19] B.T. Mott, R.S. Ferreira, A. Simeonov, A. Jadhav, K.K.-H. Ang, W. Leister, et al., Identification and optimization of inhibitors of Trypanosomal cysteine proteases: cruzain, rhodesain, and TbCatB, *J. Med. Chem.* 53 (2010) 52–60.
- [20] O. Méndez-Lucio, J. Pérez-Villanueva, A. Romo-Mancillas, R. Castillo, 3D-QSAR studies on purine-carbonitriles as cruzain inhibitors: comparative molecular field analysis (CoMFA) and comparative molecular similarity indices analysis (CoMSIA), *Med. Chem. Commun.* 2 (2011) 1058–1065.
- [21] A. Becke, Density-functional thermochemistry. III. The role of exact exchange, *J. Chem. Phys.* 98 (1993) 5648.
- [22] C. Lee, W. Yang, R.G. Parr, Development of the Colle–Salvetti correlation-energy formula into a functional of the electron density, *Phys. Rev. B* 37 (1988) 785.
- [23] L. Simon, J.M. Goodman, How reliable are DFT transition structures? Comparison of GGA, hybrid-meta-GGA and meta-GGA functionals, *Org. Biomol. Chem.* 9 (2011) 689–700.
- [24] M.J. Frisch, G.W. Trucks, H.B. Schlegel, G.E. Scuseria, M.A. Robb, J.R. Cheeseman, et al., Gaussian 09, Revision A.1, Gaussian, Inc., Wallingford, CT, 2009.
- [25] R.G. Parr, W. Yang, Density functional approach to the frontier-electron theory of chemical reactivity, *J. Am. Chem. Soc.* 106 (1984) 4049–4050.
- [26] J.L. Gázquez, Perspectives on the density functional theory of chemical reactivity, *J. Mex. Chem. Soc.* 52 (2008) 3–10.
- [27] M. Boháč, Y. Nagata, Z. Prokop, M. Prokop, M. Monincová, M. Tsuda, et al., Halide-stabilizing residues of haloalkane dehalogenases studied by quantum mechanic calculations and site-directed mutagenesis, *Biochemistry* 41 (2002) 14272–14280.
- [28] E. Dyguda, B. Szefczyk, W. Sokalski, The mechanism of phosphoryl transfer reaction and the role of active site residues on the basis of ribokinase-like kinases, *Int. J. Mol. Sci.* 5 (2004) 141–153.
- [29] P. Banáš, M. Otyepka, P. Jeřábek, M. Petřek, J. Damborský, Mechanism of enhanced conversion of 1,2,3-trichloropropane by mutant haloalkane dehalogenase revealed by molecular modeling, *J. Comput.-Aided Mol. Des.* 20 (2006) 375–383.
- [30] H. Yu, J. Liu, Z. Shen, Modeling catalytic mechanism of nitrile hydratase by semi-empirical quantum mechanical calculation, *J. Mol. Graphics Modell.* 27 (2008) 522–528.
- [31] M. Prokop, J. Adam, Z. Kriz, M. Wimmerova, J. Koca, TRITON: a graphical tool for ligand-binding protein engineering, *Bioinformatics* 24 (2008) 1955–1956.
- [32] C.G. Broyden, The convergence of a class of double-rank minimization algorithms, *J. Inst. Math. Appl.* 6 (1970) 222–231.
- [33] R. Fletcher, A new approach to variable metric algorithms, *Comput. J.* 13 (1970) 317–322.
- [34] D. Goldfarb, A family of variable-metric methods derived by variational means, *Math. Comput.* 24 (1970) 23–26.
- [35] D.F. Shanno, Conditioning of Quasi-Newton methods for function minimization, *Math. Comput.* 24 (1970) 647–656.
- [36] MOPAC2009, James J.P. Stewart, Stewart Computational Chemistry, Colorado Springs, CO, USA, <http://OpenMOPAC.net>, 2008.
- [37] J.J.P. Stewart, Optimization of parameters for semiempirical methods V: modification of NDDO approximations and application to 70 elements, *J. Mol. Model.* 13 (2007) 1173–1213.
- [38] J.J.P. Stewart, Application of the PM6 method to modeling proteins, *J. Mol. Model.* 15 (2009) 765–805.
- [39] J.J.P. Stewart, Application of localized molecular orbitals to the solution of semiempirical self-consistent field equations, *Int. J. Quantum Chem.* 58 (1996) 133–146.
- [40] J.J.P. Stewart, Calculation of the geometry of a small protein using semiempirical methods, *J. Mol. Struct.: Theochem.* 401 (1997) 195–205.
- [41] A. Klamt, G. Schuurmann, COSMO – a new approach to dielectric screening in solvents with explicit expressions for the screening energy and its gradient, *J. Chem. Soc., Perkin Trans. 2* (1993) 799–805.
- [42] G.N. Sastry, T. Bally, V. Hroudá, P. Cársky, The  $\text{C}_4\text{H}_6^{+}$  potential energy surface. 1. The ring-opening reaction of cyclobutene radical cation and related rearrangements, *J. Am. Chem. Soc.* 120 (1998) 9323–9334.
- [43] J. Moon, R. Coleman, R. Hanzlik, Reversible covalent inhibition of papain by a peptide nitrile Carbon-13 NMR evidence for a thioimidate ester adduct, *J. Am. Chem. Soc.* 108 (1986) 1350–1351.